Wall-Adapting Local Eddy-Viscosity models for simulations in complex geometries

F. Ducros F. Nicoud T. Poinsot
CERFACS, 42, Avenue Gaspard Coriolis, 31057 Toulouse cedex, France.

1 Introduction

Large-Eddy Simulations (LES) are developed to investigate the instantaneous three-dimensional structure of turbulent flows. Not only qualitative but quantitative results are now expected from these approaches both for simple and complex geometries. However, typical numerical and subgrid-scale parametrization requirements usually satisfied for the simulation of turbulent flows in simple geometries may no longer be achieved for LES in complex geometries. This leads to difficulties when LES developed for simple academic flows must be used for real flows in complex geometries. On the other hand, a short overview of industrial-type applications of LES shows what a proper LES for realistic aeronautical flows should at least do: provide a local eddy-viscosity, able to switch off during the early stages of transition and offering a proper wall scaling to get a good prediction of friction coefficient.

The objectives of the present effort are to give some elements for such a modeling.

2 Classical modeling

In LES for incompressible flows, scales smaller than the grid size are not resolved but accounted for through the subgrid scale tensor T_{ij} given by $T_{ij} = \overline{u}_i\overline{u}_j - \overline{u_i u_j}$. Most subgrid scale modeling are based on an eddy-viscosity assumption to model the subgrid scale tensor:

$$T_{ij} - \frac{1}{3}T_{kk}\delta_{ij} = 2\nu_t\overline{S}_{ij}, \quad \overline{S}_{ij} = \frac{1}{2}\left(\frac{\partial\overline{u}_i}{\partial x_j} + \frac{\partial\overline{u}_j}{\partial x_i}\right) \quad . \tag{2.1}$$

Modeling the subgrid-scale tensor in the spectral space with the same assumption leads to ν_t as $\nu_t(k,m) = \nu_t^+(k,m)\sqrt{\frac{E(k_c,t)}{k_c}}$, $E(k_c,t)$ is the cutoff kinetic energy, $k_c = \frac{\pi}{\Delta}$ is the cutoff wavenumber. ν_t^+ is an increasing function of k accounting for a cusp-behaviour near the cutoff and a decreasing function of m, the slope of the kinetic energy spectrum: $E(k) \propto k^{-m}$ (see [5]). The form $\nu_t(k,m)$ has two interesting properties: ν_t is zero as soon as there is no energy near the cutoff, that is for transitional state and ν_t decreases near walls since the slope m is larger in the wall than in the core regions of boundary layer. A simplified version of $\nu_t^+(k,m)\sqrt{\frac{E(k_c,t)}{k_c}}$ is used to get ν_t in physical space. Assuming that ν_t does no longer depend on k and provides the same dissipation ϵ as an isotropic incompressible turbulence leads to

$$\epsilon = 2\nu_t\int_0^\infty k^2E(k)dk, \quad \epsilon = 2\nu_t < \overline{S}_{ij}\overline{S}_{ij} > \quad , \tag{2.2}$$

$<>$ standing for an average on the whole physical domain. Using $E(k) = C_K\epsilon^{2/3}k^{-5/3}$ ($C_K \approx 1.4$ is the Kolmogorov constant) in eq. 2.2 gives

$$\nu_t = \frac{2}{3}C_K^{-3/2}\sqrt{\frac{E(k_c)}{k_c}} \quad . \tag{2.3}$$

Since the cusp behaviour and the dependence on m are forgotten, the physical reasons accounting for damping of ν_t near wall regions are no longer contained in the model.
Coming back to physical space requires to express eq. 2.3 with a local operator leading to models of the generic forms:

$$\nu_t = C_1 \Delta \sqrt{\overline{OP_1}(\vec{x},t)} \quad or \quad \nu_t = (C_2\Delta)^2 \sqrt{\overline{OP_2}(\vec{x},t)}. \tag{2.4}$$

Δ is a characteristic length scale of the cutoff length scale. C is determined by a relation of following type (requiring isotropy):

$$< \overline{OP}_{i\vec{x}} >= \int_0^{k_c} \Phi(E(k),k)dk, \quad i \in [1,2]. \tag{2.5}$$

$\Phi(E(k),k)$ being a function of $E(k)$ and k. $E(k_c)$ is determined with the aid of 2.5, which gives $E(k_c) = \mathcal{F}(< \overline{OP_i} >)$, which is plunged in eq. 2.3 to get C_i when comparing eq. 2.3 and eq. 2.4. This process covers a set of several models, each based on a different invariant (see also table 1):

- $\overline{S}_{ij}\overline{S}_{ij}$, for Smagorinsky's model,
- $\overline{F}_2(r)$, for the structure function model. A distinction is classically made within four- $\overline{F4}_2$ and six- $\overline{F6}_2$ point formulation

$$\overline{F6(\vec{x})}_2(r) = \frac{1}{6}\sum_{i=1}^{3} ||\vec{u}(\vec{x}) - \vec{u}(\vec{x}+\Delta x_i\vec{e}_i)||^2 + ||\vec{u}(\vec{x}) - \vec{u}(\vec{x}-\Delta x_i\vec{e}_i)||^2 \quad , \tag{2.6}$$

$$\overline{F4(\vec{x})}_2(r) = \frac{1}{4}\sum_{i=1}^{2} ||\vec{u}(\vec{x}) - \vec{u}(\vec{x}+\Delta x_i\vec{e}_i)||^2 + ||\vec{u}(\vec{x}) - \vec{u}(\vec{x}-\Delta x_i\vec{e}_i)||^2 \quad , \tag{2.7}$$

  $\overline{F4(\vec{x})}_2(r)$ being evaluated in directions parallel to the wall.

The basic structure function and Smagorinsky's models are now well known ([5],[9]). In order to get rid of the large scales responsible for spurious contribution in the evaluation of ν_t and to construct a better evaluation of $E(k_c)$, the same operators have been defined on high-pass filtered velocity fields, giving:

- $HP(\overline{F}_2 p)(r) = ||HP(\vec{\overline{u}}(\vec{x}+\vec{r},t)) - HP(\vec{\overline{u}}(\vec{x},t))||^2$ for the filtered structure function model [2],
- $HP(\overline{S_{ij}}) = \frac{1}{2}\left(\frac{\partial HP(\overline{u}_i)}{\partial x_j} + \frac{\partial HP(\overline{u}_j)}{\partial x_i}\right)$ for the filtered Smagorinsky's model [3].

$HP(\overline{u}_j)$ is obtained by applying a high-pass filter on the resolved velocity fields. The filtering process is quite arbitrary. However, it can be shown that standard centered differencing leads to filters of transfer function of the following form $\frac{E_{HP}(k)}{E(k)} = a\left(\frac{k}{k_c}\right)^b$, leading to specific constant $C(a,b)$ (see table 1). In practice, the eddy-viscosity is made local by forgetting the average $<>$, which leads to the expression 2.4.

3 An alternative operator

For reasons connected with the wall behaviour of the subgrid-scale model (see section 5), we define a new operator based on the traceless symmetric part of the square of the gradient velocity tensor $\overline{g}_{ij} = \frac{\partial u_i}{\partial x_j}$:

$$\mathcal{S}^d_{ij} = \frac{1}{2}\left(\overline{g}^2_{ij} + \overline{g}^2_{ji}\right) - \frac{1}{3}\delta_{ij}\overline{g}^2_{kk}, \tag{3.1}$$

$< \overline{OP} >_{\vec{x}}$	$\Phi(E(k),k)$	$C_{theoretical}$	$\frac{\nu_t}{\sqrt{(<\overline{OP}>}}$
$< \overline{Fp}_2(r) >$	$4k^2E(k)s_{c1}(k\Delta)$	$\frac{1}{3\pi^{4/3}}C_K^{-3/2}C_0^{-1/2}$	0.063Δ
$2 < \overline{S}_{ij}\overline{S}_{ij} >$	$k^2E(k)$	$\frac{1}{\pi}\left(\frac{3C_K}{2}\right)^{-3/4}$	$(0.18\Delta)^2$
$< HP(\overline{F}p_2) >$	$4k^2E_{HP}(k)s_{c1}(k\Delta)$	$\frac{1}{3\pi^{4/3}}C_K^{-3/2}C_b^{-1/2}\left(\frac{\pi^b}{a}\right)^{1/2}$	$C_{f,\mathcal{F}}(a,b)\Delta$
$2 < HP(\overline{S_{ij}})HP(\overline{S_{ij}}) >$	$k^2E_{HP}(k)$	$\frac{1}{\pi}\left(\frac{3C_K}{2}\right)^{-3/4}\left(\frac{4a}{3b+4}\right)^{-1/4}$	$(C_{s,\mathcal{F}}(a,b)\Delta)^2$

Table 1: $\overline{Fp}$ and $HP(\overline{F}p)$ stands for six and four-point formulation, $s_{c1}(x) = 1 - sinx/x$, $C_b = \int_0^\pi x^{-5/3+b}sin_{c1}(x)dx$.

where $\overline{g}_{ij}^2 = \overline{g}_{ik}\overline{g}_{kj}$. The second invariant of this tensor is proportional to $\overline{OP} = \mathcal{S}_{ij}^d\mathcal{S}_{ij}^d$. We cannot connect any average of this operator with the kinetic energy spectrum as proposed in 2.5. However, this operator can be used in the form $\nu_t = (C\Delta)^2\psi(\overline{OP})$, ($\psi(\overline{OP})$ is homogeneous to a frequency) the constant C being numerically evaluated so that the use of ν_t produce the same average dissipation as in 2.2 when using the Smagorinsky's model for example. This leads to

$$C^2 = C_s^2\frac{\sqrt{2} < \left(\overline{S}_{ij}\overline{S}_{ij}\right)^{3/2} >}{< \psi(\overline{OP})\overline{S}_{ij}\overline{S}_{ij} >} \tag{3.2}$$

4 Operators as function of strain and rotation rate

Operators are supposed to act locally where small scales responsible for dissipation take place. Developing the structure function in function of $\overline{S}_{ij}$ and $\overline{\Omega}_{ij} = \frac{1}{2}\left(\frac{\partial\overline{u}_i}{\partial x_j} - \frac{\partial\overline{u}_j}{\partial x_i}\right)$ when using first order velocity derivatives gives (for the six-point formulation, see [1])

$$< \overline{F}_2(r) >= \left(\frac{\Delta^2}{3}\right)\sqrt{2S^2 + \Omega^2 + \mathcal{O}(\Delta^2)} \quad , S^2 = \overline{S}_{ij}\overline{S}_{ij}, \quad \Omega^2 = \overline{\Omega}_{ij}\overline{\Omega}_{ij}. \tag{4.1}$$

Making use of the Cayley-Hamilton theorem, the operator $\overline{OP} = \mathcal{S}_{ij}^d\mathcal{S}_{ij}^d$ can be developed as:

$$\mathcal{S}_{ij}^d\mathcal{S}_{ij}^d = \frac{1}{6}\left(S^2S^2 + \Omega^2\Omega^2\right) + \frac{2}{3}S^2\Omega^2 + 2IV_{S\Omega}, \quad IV_{S\Omega} = \overline{S}_{ik}\overline{S}_{kj}\overline{\Omega}_{jl}\overline{\Omega}_{li} \tag{4.2}$$

From relations 4.2 and 4.1, a LES model based on $\mathcal{S}_{ij}^d\mathcal{S}_{ij}^d$ or on $\overline{F}_2$ will detect turbulence structures with either (large) strain rate, rotation rate or both, in agreement with more probable localisation of dissipation [11]. In the particular case of pure shear (e.g. $\overline{g}_{ij} = 0$ except $\overline{g}_{12}$), we get $S^2 = \Omega^2 = 4\overline{S}_{12}$ and $IV_{S\Omega} = -\frac{1}{2}S^2S^2$ so that $\mathcal{S}_{ij}^d\mathcal{S}_{ij}^d$ is zero: this means that almost no eddy-viscosity would be produced in the case of a wall-bounded laminar flow by a model using $\mathcal{S}_{ij}^d\mathcal{S}_{ij}^d$. Thus the amount of turbulent diffusion would be negligible and allows the development of linearly unstable waves, as filtered operators do. This is a great advantage over the non-filtered operators.

5 Behaviour of the operators for wall bounded flows

If y is the direction normal to a wall, the expansion of the subgrid scale tensor in the limit $y \simeq 0$ and $y > 0$ shows that $lim_{y\longrightarrow 0}T_{ij} = O(y^3)$. As the behaviour of $\overline{S}_{ij}$ is of order $O(1)$ in the same limit, it is classically admitted that the eddy-viscosity ν_t should scale in

$O(y^3)$. Assuming that the cutoff lenght Δ plays no important roles in the behaviour of ν_t near the wall and that the constants C remains constant, none of the previous operator does exhibit the proper behaviour (see table 2). A proper behaviour for ν_t near the wall can be

$\overline{OP}$	$lim_{y\longrightarrow 0}\overline{OP}(y)$
$<\overline{F6}_2(r)>$	$O(1)$
$2<\overline{S}_{ij}\overline{S}_{ij}>$	$O(1)$
$<HP(\overline{F6}_2)>$	$O(1)$
$2<HP(\overline{S}_{ij})HP(\overline{S}_{ij})>$	$O(1)$
$<\overline{F4}_2(r)>$	$O(y^2)$
$<HP(\overline{F}4_2)>$	$O(y^2)$
$\mathcal{S}^d_{ij}\mathcal{S}^d_{ij}$	$O(y^2)$

Table 2: Wall behaviour of the classical operators used for subgrid scale modeling

obtained in a very pragmatic manner using a damping law of Van-Driest type. However, this procedure requiring the knowledge of the friction coefficient and of the wall position encounters strong limitations. A way to get a proper scaling consists in combining some of the previous operators of different behaviour. Here are two examples (among many):

• **Adapted Filtered Structure Function**

$$\nu_t = C\Delta\left(HP(\overline{F}_2)\right)^{1/2}\left(\frac{2(\overline{F4}_2)}{\overline{F4}_2+\overline{F6}_2}\right) \tag{5.1}$$

C is consistant with the theoretical determination of the constant obtained for the standard filtered model, because the wall correction $2(\overline{F4}_2)/(\overline{F4}_2+\overline{F6}_2)$ is about 1 for isotropic turbulence. This models provides good results on coarse grid for boundary layers, see [10].

• **WALE model**

$$\nu_t = (C_m\Delta)^2\frac{\left(\mathcal{S}^d_{ij}\mathcal{S}^d_{ij}\right)^{3/2}}{\left(\overline{S}_{ij}\overline{S}_{ij}\right)^{5/2}+\left(\mathcal{S}^d_{ij}\mathcal{S}^d_{ij}\right)^{5/4}}, \tag{5.2}$$

C_m is obtained using the relation 3.2, which gives, for a collection of isotropic turbulent fields obtained with various resolutions, $C_m^2 \approx 10.6C_s^2$ ([6]). Both models 5.1 and 5.2 are local, have a proper behaviour near the wall, and are defined to handle with transitional problem in parietal flow.

6 Results

The Standard Smagorinsky's, Filtered Smagorinsky's (FiSm) and the WALE models have been implemented in a code based on the *COUPL* [1] software library that has been developed at CERFACS and Oxford University [8]. This library uses cell-vertex finite-volume techniques based on arbitrary unstructured and hybrid grids to solve the three-dimensional compressible Navier-Stokes equations. It has already been successfully used to perfom LES [7, 3].

This numerical tool has been used for the simulation of a turbulent pipe flow in the same configuration as in [6], [3] for the FiSm and the WALE models. The pipe radius is R, its

[1] Cerfacs and Oxford University Parallel Library

length $4R$, it is periodic in the streamwise direction x. The Mach number is about 0.25 and the Reynolds number based on the bulk velocity U_b is $R_b = 10000$ ($R^+ \simeq 320$ based on the friction velocity and the pipe radius). The simulations have been performed using a hybrid mesh with structured hexahedral cells near the wall and prisms in the core region. The resolution is about $\delta_x^+ \simeq 28$, $\delta r^+ \simeq 2.1$ (at the wall) and $R\delta_\theta^+ \simeq 8.8$ in the streamwise, radial and azimuthal directions respectively. The initial condition consists of a Poiseuille flow superimposed to a white noise of small amplitude (0.1%). A source term is added to the Navier-Stokes equations to simulate a pressure gradient corresponding to the fully turbulent state. Transition to turbulence occurs for both FiSm and WALE models, before a statistically steady state is reached (see details in [6]).

Profiles of streamwise velocity obtained with both models are plotted in figure 1. For $y^+ > 30$, our results exhibit the classical logarithmic law almost up to the centerline of the pipe flow, as expected from published results [4]. Results obtained with WALE suggest 0.416 for the Von Karman's constant κ and $C \simeq 5.$, which is in the common range for turbulent velocity profiles. Smaller values of the constants are representative of FiSm results ($\kappa = 0.39$, $C \simeq 4.5$). Streamwise and radial fluctuation velocities are compared with the available PIV measurements [4] at a lower Reynolds number ($R_b = 5450$). The location and the level of the maximum of the turbulence intensity in the streamwise direction are well predicted by the computations. The WALE model produces a level of radial fluctuations slightly lower, which is in better agreement with the experimental data.

The curves in figure 2 have been obtained by applying the classical Smagorinsky's, the FiSm, and the WALE models to a turbulent field obtained with the WALE model. For the WALE model, ν_t is of order r^3 near the pipe wall, confirming its proper scaling. The eddy-viscosity is two orders of magnitude smaller than the molecular viscosity in the sublayer. Both the Smagorinsky's and the FiSm models produce a large amount of eddy-viscosity at the wall. For the Smagorinsky's model, this leads to a complete relaminarization. For the FiSm model, the wrong behaviour at the wall reduces the effective Reynolds number so that only 85 % of the expected mass flow rate in the pipe was obtained. The correct bulk velocity has been reached with the WALE formulation. Note also from figure 2 that the three models lead to similar eddy-viscosity in the core region of the pipe, where the turbulence is nearly isotropic.

Different visualisations of instantaneous 3D fields have been also performed. Evidences of turbulent motions at very small scales near the wall can be observed. In the core region of the pipe, the turbulence develops at a larger scale, justifying the use of larger prismatic cells near the centerline (see Fig. 2).

7 Conclusion

An analysis of the behaviour of the more often used invariants for LES applications is proposed. A new operator based on the square of the gradient velocity tensor is proposed and shown to behave in y^2 near a wall. A general way to build operators having a proper behaviour in the case of wall-bounded flow is proposed. Two new models are proposed to illustrate this methodology, leading to an adaptation of the filtered structure function model and to the Wall Adapted Local Eddy viscosity model. The latter is used to perform the transition to turbulence of the flow is a pipe on an unstructured grid. These results are compared with previous calculations obtained with the filtered Smagorinsky's model and are shown to improve the prediction of the wall stress rate, as well as turbulent intensities.

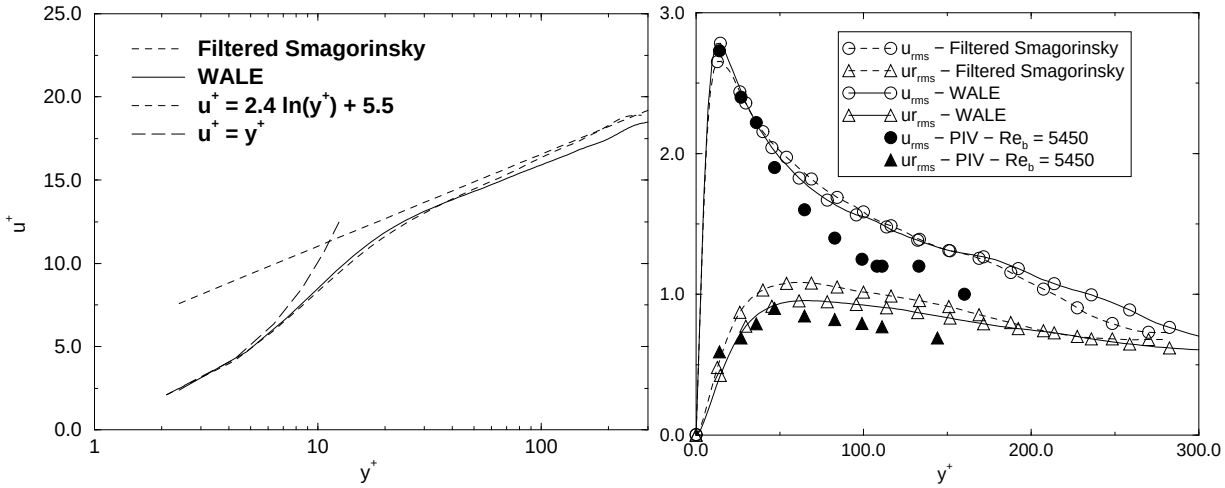

Figure 1: Comparison between FiSm and WALE results: **left:** Mean velocity profiles in semi-log coordinates, plus the laws $u^+ = y^+$ and $u^+ = \frac{1}{\kappa} ln(y^+) + C$, **right:**Root-mean-square streamwise and normal velocity. Comparison between the filtered-Smagorinsky model and the WALE formulation. Experimental data from Eggels et al. (see also [6]).

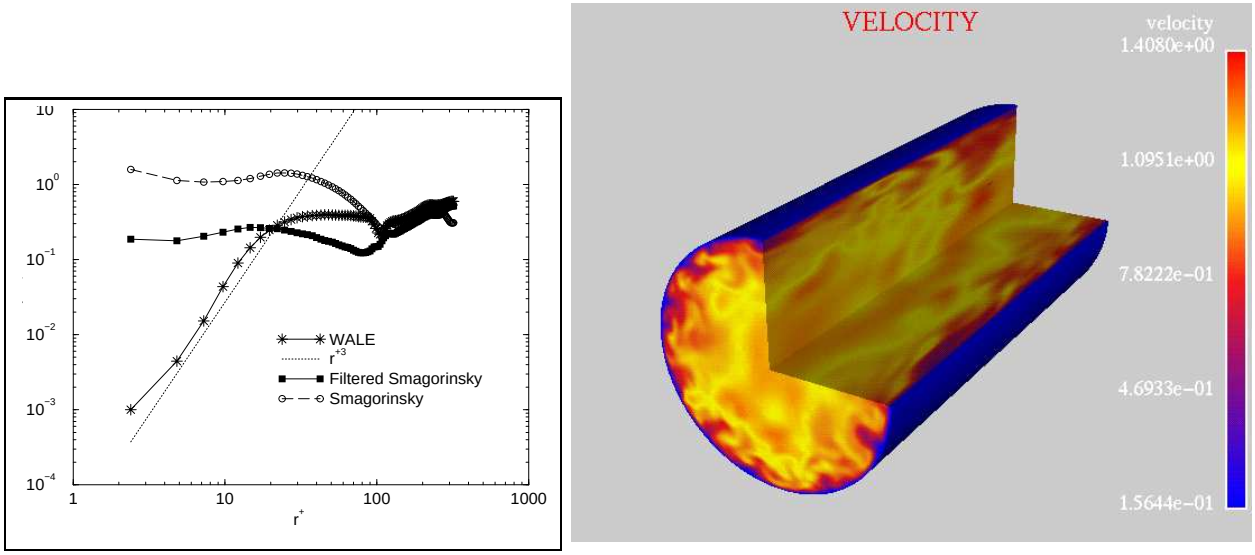

Figure 2: **left:**Ratio of average eddy-viscosity to molecular viscosity in log-log coordinates. Comparison between the classical Smagorinsky model, its filtered version and the WALE model. **right:** cut in the total velocity for a turbulent state.

References

[1] P. Comte, F. Ducros, J. Silvestrini, E. David, E. Lamballais, O. Métais, and M. Lesieur. Simulation des grandes échelles d'écoulements transitionnels. *AGARD Conference proceedings 551*, pages 14–1/14–11, 1994.

[2] F. Ducros, P. Comte, and M. Lesieur. Large-eddy simulation of transition to turbulence in a boundary layer spatially developing over a flat plate. *Journal of Fluid Mechanics*, 326:1–36, 1996.

[3] F. Ducros, F. Nicoud, and T. Schonfeld. Large-eddy simulation of compressible flows on hybrid meshes. *Eleventh Symposium on Turbulent Shear Flows, Grenoble, France*, 3:28–1, 28–6, 1997.

[4] J.G.M. Eggels, F. Unger, M.H. Weiss, J. Westerweel, R.J. Adrian, R. Friedrich, and F.T.M. Nieuwstadt. Fully developed turbulent pipe flow: a comparison between direct numerical simulation and experiment. *Journal of Fluid Mechanics*, 268:175–209, 1994.

[5] M Lesieur and O. Métais. New trends in large-eddy simulations of turbulence. *Annual Rev. Fluid Mech.*, 28:45–82, 1996.

[6] F. Nicoud and F. Ducros. Subgrid-scale stress modelling based on the square of the velocity gradient tensor. *submitted to Flow, Turbulence and Combustion.*, 1998.

[7] F. Nicoud, F. Ducros, and T. Schoenfeld. Towards direct and large eddy simulations of compressible flows in complex geometries. *To appear in Notes in Numerical Fluid Mechanics, Vieweg*, December 1997.

[8] M. Rudgyard, T. Schoenfeld, R. Struijs, and G. Audemar. A modular approach for computational fluid dynamics. *Proceedings of the 2nd ECCOMAS–Conference,Stuttgart*, 1994. Also exists as CERFACS Technical Report TR/CFD/95/07.

[9] J. Smagorinsky. General circulation experiments with the primitive equations, i, the basic experiment. *Mon. Weather Rev.*, 92, 1963.

[10] C. Weber, F. Ducros, and A. Corjon. Large-eddy simulation of complex turbulent flows. *AIAA Paper 98-2651*, 1998.

[11] A.A. Wray and J.C.R. Hunt. Algorithms for classification of turbulent structures. *Topological Fluid Mechanics, Proceedings of the IUTAM Symposium*, pages 95–104, 1989.